Ultrasonic free fatty acids esterification in tobacco and canola oil

D.C. Boffito*[,a,b], F. Galli[a], C. Pirola[a], C.L. Bianchi[a], G.S. Patience[c]

[a]Università degli Studi di Milano ' Dipartimento di Chimica, via Golgi 19, 20133 Milano, Italy

[b] currently at [c] Polytechnique Montréal – Departement de Génie Chimique, 2900 Édouard-Montpetit, 2500 Chemin Polytechnique, H3T 1J4 Montreal

*corresponding author: daria-camilla.boffito@polymtl.ca

Abstract

Ultrasound accelerates the free fatty acid esterification mass transfer. The reaction rates of tobacco seed oil, canola oil and oleic acid increase in a batch reactor and in presence of the heterogeneous catalyst Amberlyst®46. The beneficial effects of ultrasound vs. the conventional approach are more marked at lower temperatures (20 °C and 40°C vs. 63 °C): at 20 °C, the free fatty acids conversion reaches 68% vs. 23 % with conventional mechanical stirring. The enhanced conversion is attributed to acoustic cavitation that increases mass transfer in the vicinity of the active sites. The Eley-Rideal kinetic model in which the concentration of the reacting species is expressed taking into account the mass transfer between the phases is in excellent agreement with the experimental data. Ultrasound increases the mass transfer coefficient in the tobacco oil 6 and 4.1 folds at 20 °C and 40 °C, respectively.

Keywords: esterification; free fatty acids; acoustic cavitation; mass transfer; Amberlyst®46; Eley-Rideal kinetic model

1. Introduction

Abbreviations: BD: Biodiesel; FFA: Free fatty acids; ME: Methyl ester; US: Ultrasound

The search for alternative and clean energy sources has driven the scientific community to focus on synthesizing fuels from organic substrates. Among the sources of biomass-derived fuels [1-4], one is represented by the raw oils to produce biodiesel (BD). BD is a biofuel that is defined as fatty acid methyl ester derived from greases of vegetable, animal or wastes [5-7].

The synthesis of BD became a commercial reality a few decades ago [8]. However, commercial BD plants suffer from several drawbacks. The main issues are: very long processing times (up to 8 hours per batch), limited feedstock and disposal of the homogeneous (basic) catalyst [9]. A free fatty acid content (FFA) greater than 0.5 $\%_{wt}$ exceeds the European norm on biodiesel fuel (EN 14214), but also will generate a considerable amount of soap reacting with the alkaline transesterification catalyst [9 – 11]. Water can further react with the triglycerides forming FFA. High FFA and water concentrations are likely for raw or used oils. Removing FFA before the transesterification is a solution to avoid saponification during the BD production [4, 7, 10-14]. Esterification is preferred over other methods to remove FFA such as distillation or adding alkaline catalyst in excess [6, 7], since it produces methyl esters (ME), i.e. BD already at this stage. However, the oil- methanol system composing the reaction mixture of both the transesterification and esterification suffer from mass transfer limitations due to the high viscosity of the oil and the limited miscibility of the methanol and the oil [11, 15].

The challenges concerning BD production are: i) designing a heterogeneous catalyst whose activity is equal to or exceeds homogeneous systems ii) BD process intensification to maximize mass transfer rates iii) use of non-edible oils or waste oils not in competition with food iv) efficient pre-processing steps (degumming, dehydration, etc.).

Recently, many researchers have used ultrasound (US)- assisted techniques to promote and reduce reaction times of both the transesterification [16-24] and esterification [16, 17, 25, 26] reactions.

Acoustic cavitation-based technologies (such as US) have been regarded as a means to eliminate or minimize mass-transfer limitations [16-25]. Cavitation is a phenomenon of nucleation, growth, and subsequent collapse (quasi-adiabatic) of micro bubbles in a liquid medium. The collapse of bubbles

forms hot spots characterized by very high temperatures (in the range of 1000−15000 K) and pressures (in the range of 500−5000 bar) locally but at millions of locations in the reactor. In addition to the generation of hotspots, cavitation may also generate highly reactive free radicals and turbulence. When a cavitation bubble collapses near a solid surface, liquid jets are produced and high-speed jets of liquid are driven into the surface of a particle (due to asymmetric collapse of bubbles), resulting in enhanced transport of the species towards the solid surface [27]. For this reason US has been adopted extensively to promote various reactions, among which also heterogeneously-catalysed processes [28].

In the presence of two immiscible liquids, US forms fine emulsions, thereby increasing the surface area available for the reaction between the two phases. The cavitation may also lead to a localized increase in temperature at the phase boundary. As a consequence, both mass transfer rates and global reaction rate increase [29]. Emulsions produced by sonication are also reported to be more stable than those formed conventionally [30].

In this manuscript, we present the results of the ultrasonic FFA esterification of raw tobacco seed oil, refined canola oil and pure oleic acid in presence of acid ion exchange resins and compare the FFA conversions with the conventional method. This study includes a kinetic model that takes into account of the mass transfer at the phase boundaries in the reaction system methanol-oil (+FFA)-catalyst. Mass transfer has been largely ignored in the scientific literature.

2. Materials and Methods

2.1. Materials

Three feedstocks were tested including raw tobacco seed oil, canola oilseed acidified with oleic acid and pure oleic acid. The acidic composition of the oils (Table 1), i.e. the $\%_{wt}$ of each single fatty acid composing the side chains of the triglycerides for tobacco and canola seed oils or consisting in

the feedstock itself in the case of oleic acid, was determined by GC-FID after transesterification, according to the UNI EN 14103 norm [21].

Average molecular weight of the FFA in the tobacco seed oil was calculated from the acidic composition as follows:

$$\overline{MW} = \sum MW_i \times A_i \quad (1)$$

where MW_i is the molecular weight and A_i the percentage of each fatty acid.

Tobacco is a non-edible crop that has limited water needs and has proven to be a sustainable feedstock for biodiesel production. According to a preliminary life cycle assessment (LCA), adequate land management and innovative agronomic techniques resulted in a 30 % reduction of CO_2 emissions to soybean in the agronomic phase grown on marginal Italian land [31].

Tobacco seeds were pressed in extra-virgin conditions by TopAgri (Verona, Italy). The natural acidity of tobacco seed oil was 1.15%. It was more viscous than commercial oils and was filtered under vacuum before the experiments to reduce sediment, which may account for the higher viscosity. After filtration, the viscosity was sensibly unaltered.

The canola oil was a refined, edible oil and was acidified with pure oleic acid before each test (Table 2). Oleic acid (Sigma Aldrich, > 99%) and anhydrous methanol (Sigma Aldrich, > 99.8%, H_2O < 0.002%) were used without further purification.

The molecular weights of the FFA in canola oil and oleic acid was considered equal to 282.47.

Karl Fischer analyses were conducted in a dead-stop automatic titrator (Amel, model 231) using toluene as a solvent.

2.2. Catalyst Amberlyst®46

Acid ion exchange resin Amberlyst®46 (A46) was used for the experiments. It demonstrated high mechanical and chemical stability over several esterification cycles. A46 is a copolymer of styrene

cross-linked with divinylbenzene (DVB) with sulphuric type acid groups in the form of spherical beads (Figure 1). The amount of crosslinking determines its main physical characteristics (surface area and pore size distribution) (Table 3) [32]. The higher the DVB amount added during the copolymerization, the higher the reticulation degree and, as a consequence, the smaller the pores. The amount of DVB plays a major role in controlling the physical features of these catalysts (Table 3). The strong $–SO_3H$ acid groups formed on the resin during the sulphonation step are the active sites responsible for the esterification of the FFA.

The distinguishing feature of this resin is that it is sulphonated only on the surface and not inside the pores [11, 13, 14]. Being sulphonated only superficially, this type of catalyst greatly reduces the formation of dialkyl ethers given by the auto-condensation of the molecules of the alcohol inside the pores [33].

The presence of catalytically active sites mostly located on the catalyst outer surface is desirable with respect to the reaction system under study. FFA is a highly sterically hindered molecule that would hardly penetrate inside the catalysts pores [10-14]. Moreover, A46 has proven to provide constant activity in the FFA esterification, being both chemically and mechanically stable for over 90 cycles and 540 hours [14].

2.3. Esterification experiments

Esterification experiments were conducted in a 500 mL cylindrical Pyrex flask (Fig. 2) through which a titanium US horn protruded through its side horizontally. The detailed description of the reactor system, including the explanation of the special design and the energetic consideration are extensively described by Ragaini and co-authors [34]. The fluid-catalyst slurry was continuously stirred either with a magnetic bar (in the case of the conventional process) or by means of ultrasound. The vessel was maintained under iso-thermal conditions via an exterior coil wrapped

around it with glycol as the cooling (or heating) medium. A thermometer entering one of the ports at the top of the reactor monitored temperature.

The US horn was positioned 55 mm from the bottom of the reactor. The reactor was also equipped with a microwave emitter, located at the same height of the US horn [34].

The maximum nominal power of the US horn (Bandelin, Mod. Sonoplus GM 2200 sonicator), was 295 ± 2 W, with a frequency of 20 kHz and a tip diameter of 13 mm.

For the experiment reported here, 10 g of catalyst was charged to the reactor followed by 16 g of methanol. After a 5 minute period, 100 g of oil (+ acid) was added, which gives the same ratio reported in previous studies by the authors [10-14] and corresponds to a molar oil: MeOH ratio of about 4.5. The ratio of the oleic acid to MeOH was 1.4.

The reactor was heated with the coil and once the desired temperature was reached, either the stirring (100 rpm) or the ultrasound was initiated. This point is considered as time zero of the experiment.

The US emission was determined following the standard calorimetric method [27, 35], i.e. measuring the temperature increase (ΔT), in the same vessel, of a weighted volume (116 mL) of water (116 g, 6.4 mol). The sonicator was operated at 37% of the maximum nominal power in all the experiments. The power delivered to the reaction system and resulting from the calorimetric measurements was 31.7 W. The study of FFA conversion as a function of power is out of the scope of this work.

FFA conversion was determined by withdrawing samples from the reactor at regular intervals. All the samples were centrifuged for 5 minutes at 13500 rpm and the acidity was measured by an acid-base titration [6, 7, 10-14]:

$$FFA_t = \frac{V \times \overline{MW} \times C}{W} \times 100 \quad (2)$$

where V is the volume of the alcoholic KOH solution necessary for the titration (mL), $\overline{MW}$ is the average molecular weight of the acid contained in major quantity (mg $mmol^{-1}$), C is the concentration of KOH (mmol mL^{-1}) and W is the weight of the analysed sample (mg).

The FFA conversion, i.e. the percentage of acid converted to methylester was determined as follows [6, 7, 10-14].

$$FFA\ conversion\ (\%) = \frac{FFA_{t=0} - FFA_t}{FFA_{t=0}} \times 100 \quad (3)$$

3. Results and Discussion

3.1. Comparative performance of the ultrasound-assisted method and the conventional method

FFA conversion to methyl esters is faster with ultrasound (US) compared to conventional mechanical stirring at all of the experimental conditions tested (oil, acidity, temperature). At 63 °C, FFA conversion in canola oil exceeds 90 % (Figure 3) after 6 h. It only approaches about 80 % in tobacco seed oil after the same amount of time. Oleic acid conversion reaches about 70 %. US accelerates the reaction rates considerably more at lower temperatures (Figures 4 – 5) and the benefits are also more evident at shorter reaction times: at 20 °C the FFA conversion is close to that measured for the test run at 40 °C. FFA conversion was about 45 % for all three systems with US after one hour. It took two hours to reach 45 % conversion for the oleic acid-methanol and the tobacco seed oil systems and 90 minutes for the canola oil system.

US accelerates the FFA esterification by increasing the mass transfer due to acoustic cavitation. FFA esterification can be regarded as a "dual-heterogeneous system" consisting of an oil-methanol liquid-liquid system and an oil-methanol-catalyst liquid-solid system. US has been reported to be beneficial to both kinds of heterogeneous systems [27]. Concerning the liquid-liquid methanol-oil

immiscible system, US forms a very fine emulsion of two immiscible liquids that are more stable than those generated by conventional stirring [30]. As a consequence, the surface area available for the reaction between the two phases is significantly increased and, therefore, also the reaction rate is expected to increase [29].

For the liquid–solid system, the positive effects of the acoustic cavitation are attributable to the asymmetric collapse of the bubbles in the vicinity of the solid surface. When a cavitation bubble collapses violently near a solid surface, high- speed liquid jets impinge onto the particle surface. These jets and shock waves improve the liquid–solid mass transfer [27]. As methanol is added to the system, a "wreath" forms around the catalyst particles [11, 13]. When oil is added, FFA migrates towards the surface of the catalyst due to a concentration gradient. Shock waves generated by acoustic cavitation at the liquid-solid interface increases the reaction rate, since both the oil-methanol and methanol-catalyst boundaries meet at this interface.

The acidity was reduced below the European norm of 0.5 $\%_{wt}$ in the case of both canola oil and tobacco seed oil in less than 6 hours at 63 °C either with or without US. At 40°C (Figure 2), the difference between the US-assisted and the conventional process is more pronounced and, again, higher in the case of the tobacco seed oil. At 20 °C, the sonochemically-assisted method results in a similar yield to the experiments with US at 40 °C and higher than the one at 40 °C in absence of US in the tobacco seed oil system. At 63 °C and at 40 °C the difference in conversion after 6 h in the US and mechanical stirring are 6 and 8 percentage points, respectively. It is remarkable that in presence of US at 20 °C, the FFA conversion is 3 times as high as mechanical stirring.

The initial acidity in the tobacco seed oil was just over 1.15 $\%_{wt}$ and was reduced to below the target of 0.5 $\%_{wt}$ using US at all the temperatures and with the mechanical stirring at 63°C. After 6 h and at 63 °C and US, the system essentially reached equilibrium but the conversion is much lower compared to the canola oil tests. The other conditions would still require many hours to achieve equilibrium. The lower conversion may be attributable to the presence of water in the feedstock (as much as 4000 ppm) or either to the high viscosity of the oil. In fact, although tobacco seed oil is

expected to have a lower viscosity than canola, because of the higher content of linoleic acid, the tobacco seed oil appeared very thick and consequently viscous. The higher viscosity may be due to residues form the pressing or phospholipids, which are usually present in the tobacco seed oil [37].

FFA esterification is an endothermic reaction and thus the equilibrium constant (and equilibrium conversion) increases with temperature [36].

At 63 °C (Figure 3), there is little difference between FFA conversion with the conventional method and US for canola oil, whereas for tobacco seed oil and oleic acid, it is much higher for the case of US. The same trend was observed also by Gole and Gogate [16] in an experiment with the same US frequency (20 kHz), similar powers and using H_2SO_4 as a catalyst.

The superior performance for the US with tobacco seed oil and oleic acid might be due to the higher viscosity of tobacco seed oil and oleic acid with respect to canola oil. In the case of highly viscous media, the contribution of US to mass transfer is expected to be higher.

In the US experiments at 63 °C, the thermostat was set at 40°C and the US provided the heat to achieve the desired bath temperature. In fact, after initiating the sonicator, the bath temperature reached 63 °C ± 2°C within seconds.

The lower difference in conversion at 63°C compared to 40°C may be accounted for by several phenomena. It is well known that acoustic cavitation is better at low temperatures: more gas (air) is dissolved in liquids at lower temperature and this gas generates active nuclei for acoustic cavitation. Vapour pressure increases with temperature, which enhances bubble formation; however, since the vapour pressure is higher, the bubble collapse is less violent. Also, viscosity is lower at higher temperatures, and thus mass transfer resistance for the conventional process will be lower.

3.2. Kinetic analysis

In a homogeneous system, equilibrium conversion depends on temperature and the initial concentration of reactants; the equilibrium constant depends solely on temperature. As noted above oil-methanol-catalyst is a doubly heterogeneous system. Thus, the bulk phase concentration may not

be representative of the equilibrium conversion in the boundary phase of the catalyst. Furthermore, the equilibrium is shifted if one of the products or reactants is removed from the system like adsorption of a compound to the catalyst. Assuming that equilibrium is reached at 63 °C, the apparent equilibrium constant (K_{eq}) equals 2, 0.3 and 0.02 (adimensional) for oleic acid, canola oil and tobacco seed oil, respectively. The objective of this study is to assess the degree in which the US accelerates mass transfer and not necessarily a comprehensive model to account for all of the phenomena described above. Therefore, a mass balance equation was derived considering two phases – a bulk phase for which we measured the concentrations, and a boundary phase at the surface of the catalyst. We assume that:

a) The rate of the reaction in absence of catalyst is negligible at all temperatures and for both the mechanically-stirred and the sonicated reactor.

b) The temperature is uniform.

c) The reaction starts only when the mechanical stirrer or sonicator is initiated.

d) Catalyst deactivation is negligible during the course of the experiments.

Many recent studies hold that mass transfer resistance is negligible at high stirring rates [15, 38, 39] and substantiate this postulate by demonstrating that conversion remains constant beyond a certain stirring rate. We suggest that increasing the stirring rate may reduce mass transfer resistance in the bulk but may not affect the boundary layer mass transfer or the interface between the emulsion and the catalyst active sites.

Few studies have modelled the US-assisted esterification kinetics. Several papers report that US increases mass transfer in the oil/MeOH systems, but their homogeneous kinetic models [17, 40, 41] neglect it in the overall reaction rate.

The model proposed here takes into account both the surface reaction and mass transfer between the surface and bulk phase. Initially, mass transfer is limiting but as the system approaches equilibrium, the reaction kinetics becomes slower. We assume that the esterification of the FFA follows an Eley-Ridel type reaction mechanism: FFA adsorbs onto an acidic site (X) to form an adsorbed species

$X_{FFA,s}$ (1); this species reacts with methanol and releases methyl esters (ME) to the liquid phase and forms an adsorbed water as species on the active sites X_{H2O} (2). The last step is the H_2O desorption (3).

$$C_{FFA,S} + X \leftrightarrow X_{FFA} \quad (4)$$

$$X_{FFA,S} + C_{MeOH,S} \leftrightarrow X_{H_2O} + C_{ME,S} \quad (5)$$

$$X_{H_2O} \leftrightarrow C_{H_2O,S} + X \quad (6)$$

Assuming that the surface reaction (step 2) limits the rate and that the adsorption of FFA and the desorption of water are in equilibrium, the rate equation becomes:

$$r = \frac{k\left(C_{FFA,S} \cdot C_{MeOH,S} - \frac{C_{H_2O,S} \cdot C_{ME,S}}{K_{eq}}\right)}{1 + K_1 C_{FFA,S} + K_3 C_{H_2O,S}} \quad (7)$$

The adsorption terms were neglected in the parameter estimation. This expression was combined with a mass balance between the boundary layer at the surface of the catalyst and bulk liquid:

$$\phi V \frac{d}{dt} C_i = -k_m (C_i - C_{i,s}) \quad (8)$$

where C_i and $C_{i,s}$ represent the concentration of each of the four reacting species in the bulk and on the surface of the catalyst, respectively. Mass transfer between the catalyst surface and the bulk is represented by k_m and V is the total fluid volume and ϕ is the fractional volume of the bulk phase; (1-ϕ) is the volume of the boundary layer around the catalyst.

The mass balance for water in the bulk phase becomes:

$$\phi V \frac{d}{dt} C_{H2O} = -k_m (C_{H2O} - C_{H2O,s}) - k_{H2O} C_{H2O} (C_T - C_{H2O,ads}) \quad (9)$$

The mass balance for the surface boundary layer phase is:

$$(1 - \phi) V \frac{d}{dt} C_{i,s} = k_m (C_i - C_{i,s}) - \upsilon_i r \quad (10)$$

where the stoichiometric coefficient, υ_i, equals1 for FFA and MeOH and is -1 for ME and H_2O. Finally, the mass balance around the water adsorption by the catalyst is

$$W \frac{d}{dt} C_{H2O,ads} = -k_{H2O} C_{H2O} (C_T - C_{H2O,ads}) \quad (11)$$

where W is the weight of catalyst (g), C_T, is the capacity of the catalyst to absorb water (equals 0.4 g/g catalyst) and $C_{H2O,ads}$ is the molar concentration of water on the surface. Note that the adsorbed water, $C_{H2O,ads}$, is assumed to be independent of the reaction sites. The fitted parameters include the rate constant k, the mass transfer coefficient between the boundary layer and bulk fluid, k_m, as well as the equilibrium constants, K_{eq} and the absorption coefficient k_{H2O}.

The boundary volume and mass transfer rate are coupled parameters such that an increase in one will decrease the other proportionately. Therefore, we assumed a fixed boundary thickness and combined the two terms into a single coefficient k_m. The average particle diameter was 0.85 mm and the boundary layer was assumed to equal 30 μm, which represents about 3 % of the total volume of the catalyst.

To assess the impact of the US on the reaction rate, the experiments with and without US were compared keeping the other conditions constant – type of oil, temperature and initial acidity. The type and amount of catalyst used for all the tests was the same (10 g of A46 for each 100 g of oil or oleic acid).

The conversion of FFA in the tobacco seed oil is lower compared to canola oil (Figure 3 and 4).One of the major differences is the initial FFA concentration, that is about 1 % versus the 4 % for tobacco and canola oil, respectively. However, this difference was insufficient to account for the lower conversion. US enhances the mass transfer rate considerably with the exception of the test with canola oil at 63 °C. In this case, the conversion reached 94 % after a reaction time of 6 h, whereas it only reached 91 % with US. This lower conversion must be due to equilibrium considerations – perhaps water contamination, lower temperature or MeOH might have preferentially evaporated during this test, as already hypothesized by the authors in a previous study [21]. All other tests show a significant improvement in the mass transfer rate with US – typically greater than 2X. Table 4 summarizes the relative improvement, $k_{m,US}/k_{m,}$ and the best fit parameters.

Even if several papers report that external diffusion can be neglected [15, 38, 39], the reactive system under study contains two boundaries. As a consequence, even considering that there are no

diffusion limitations in the oil phase, there are still the diffusional considerations with respect to the oil/MeOH boundary in proximity of the catalyst surface.

The oleic acid/MeOH system is a single-phase solution. Therefore we expect that the mass transfer should be due solely to the bulk phase. This test was made at the highest oleic acid concentration maintaining the same mass of MeOH as in the other experiments (100 g of oleic acid and 16 g of MeOH). However the mole fraction of MeOH is lower (0.585) compared to the tests with seed oils (0.800).

Oleic acid conversion was lower compared to most of the other experiment but its K_{Eq} was the highest. We expected that all the tests conducted at 63 °C would have had the same or similar value of the K_{Eq}. We attributed the higher value of the K_{Eq} in the oleic acid tests to the presence of water. The catalyst A46 is well known to adsorb as much as 40 % of its weight of water [11]. Subtracting water from the system shifts the equilibrium towards products and thus alters the equilibrium constant based on the bulk concentration.

Each experiment was conducted as a pair: with and without US. The rate constant, equilibrium constant for each pair were given the same value and the data was fit allowing the mass transfer coefficient to vary.

The model fits the experimental data very well with correlation coefficients greater than 0.97 and greater than 0.995 for the oleic acid tests. Nevertheless, the presence of water is problematic for the calculation of the reaction rate and the equilibrium. Any water originally present in the oil reduces the equilibrium conversion. While oleic acid is water free, Karl Fischer analysis confirmed that water originally present in canola oil is of the order of 600 ppm (and may increase with time under air exposure) and in the tobacco seed oil is as much 2000 ppm. At 63 °C the test fit value of the Keq for oleic acid was 0.57 (assuming k_{H_2O}=0.06), 0.38 and 0.05 for canola oil and tobacco oil, respectively. The presence of water undoubtedly affects the conversion at the equilibrium; however, the impact of US on the mass transfer rate is independent of the assumed initial concentration of water. For instance, increasing the initial concentration of water in the tobacco seed oil from 600, to

4000 and 10 000 ppm, increases the calculated K_{Eq} to 0.026, 0.1 and 0.28, respectively (at 63 °C). However, the mass transfer coefficient for the conventional and US process, k_m and $k_{m,US}$, remains unchanged at 0.00162 and 0.05 regardless of the amount of water with R^2>0.98. More importantly, their ratio is constant as well. Thus, we may use the model to accurately characterize the change in mass transfer rate with US.

Figures 3 to 5 demonstrate excellent agreement between the model and experimental data at 63 °C and 40 °C for the A46 catalyst and various types of oils. The model confirms that mass transfer rates are higher with US at lower temperatures. It is 6 fold higher at 20 °C with tobacco oil compared to 4X at 40 °C and only 2X at 63 °C. With the less viscous canola oil, the increase in mass transfer with US versus conventional stirring is 2.6X at 40 °C and essentially the same at 63 °C.

4. Conclusions

Ultrasound increases the conversion rate of free fatty acids (FFA) with respect to conventional mechanical stirring. In particular, de-acidification rates are much higher for oleic acid and tobacco seed oil and the accelerated rate may be due to the low mass transfer in these fluids that have a higher viscosity. The lower the temperature, the higher is the difference between the reaction rate between US and mechanical stirring: the conversion of FFA in the tobacco seed oil at 20 °C is three times higher than the conventional approach at the same temperature. FFA esterification can be characterized as a doubly-heterogeneous system with two phase boundaries: the catalyst-liquid boundary and the one between the methanol that surrounds the catalyst particle and the oil. Acoustic cavitation acts to either shrink the boundary layer or to allow the bulk reactants to penetrate to the reacting surface more quickly: mass transfer coefficients are several fold higher with US compared to mechanical stirring.

Acknowledgements

The authors gratefully acknowledge the Italian Ministry of Agriculture (project SUSBIOFUEL – D.M. 27800/7303/09) and for the financial support from the the Fonds de recherche du Québec - Nature et technologies (FQRNT) for the PBEEE Fellowship.

Bibliography

[1] S. Berzegianni, A. Dimitriadis, Comparison between different types of renewable diesel, Ren. Sus. En. Rev. 21 (2013), 110-116.

[2] F. Manenti, A. Garcon-Leon, G. Bozzano, Energy-process integration of the gas-cooled/water-cooled fixed-bed reactor network for methanol synthesis, Chem. Eng. Trans. 35, (2013) 1243-1248.

[3] F. Manenti, S. Cieri, M. Restelli, G. Bozzano, Dynamic Modelling of the Methanol Synthesis Fixed-Bed Reactor, Comp. & Chem. Eng. 48, (2013) 325-334.

[4] F. Manenti, S. Cieri, M. Restelli, Considerations on the steady-state modeling of methanol synthesis fixed-bed reactor, Chem. Eng. Sci. 66(2), (2011) 152-162.

[5] E. Lotero, Y. Liu, D.E. Lopez, K. Suwannakarn, D.A. Bruce, J.G. Goodwin, Synthesis of biodiesel via acid catalysis, Ind. Eng. Chem. Res. 44 (14), (2005), 5353-5363.

[6] C. Pirola, D.C. Boffito, G. Carvoli, A. Di Fronzo, V. Ragaini, C.L. Bianchi, Soybean oil deacidification as a first step towards biodiesel production, in: D. Krezhova (Ed.), Recent Trends for Enhancing the Diversity and Quality of Soybean Products, Intech, 2011, pp. 321-344.

[7] C.L. Bianchi, C. Pirola, D.C. Boffito, A. Di Fronzo, G. Carvoli, D. Barnabè, R. Bucchi, A. Rispoli, Non edible oils: raw materials for sustainable biodiesel in: M. Stoytcheva, G. Montero (Eds.), Biodiesel Feedstocks and Processing Technologies, Intech, 2011, pp. 3-22.

[8] B.L. Salvi, N.L. Panwar, Biodiesel resources and production technologies – A review, Ren. Sust. Energy Rev. 16 (6), (2012), 3680-3689.

[9] C. Perego, M. Ricci, Diesel fuel from biomass, Catal. Sci. Technol. 1 (2012), 1776-1786.

[10] C.L. Bianchi, D.C. Boffito. C. Pirola, V. Ragaini, Low temperature de-acidification process of animal fat as a pre-step to biodiesel production, Catal. Lett. 134 (2010) 179-183.

[11] D.C. Boffito, C. Pirola, F. Galli, A. Di Michele, C.L. Bianchi, Free fatty acids esterification of waste cooking oil and its mixtures with rapeseed oil and diesel, Fuel 108 (2012) 612-619.

[12] D.C. Boffito, V. Crocellà, C. Pirola, B. Neppolian, G. Cerrato, M. Ashokkumar, C.L. Bianchi, Ultrasonic enhancement of the acidity, surface area and free fatty acids esterification catalytic activity of sulphated ZrO_2-TiO_2 systems, J. Catal. 297 (2012) 17-26.

[13] D.C. Boffito, C. Pirola, C.L. Bianchi, Heterogeneous catalysis for free fatty acids esterification reaction as a first step towards biodiesel production, Chem. Today 30 (2012) 14-18.

[14] C. Pirola. C.L. Bianchi. D.C. Boffito, G. Carvoli, V. Ragaini, Vegetable oil deacidification by Amberlyst: study of catalyst lifetime and a suitable reactor configuration, Ind. Eng. Chem. Res. 40 (2010), 4601-4606.

[15] Y. Liu, H. Lu, C. Liu, B. Liang, Solubility measurements for the reaction systems in pre-esterification of high acid value Jatropha curcas L. Oil, J. Chem. Eng. Data 54 (2009) 1421-1425.

[16] V.L. Gole, P.R. Gogate, Intensification of synthesis of biodiesel from non edible oils using sonochemical reactors, Ind. Eng. Chem. Res. 51(37) (2012) 11866-11874.

[17] V.L. Gole, P.R. Gogate, R. Parag. A review on intensification of synthesis of biodiesel from sustainable feedstock using sonochemical reactors, Chem. Eng. Proc. 53 (2012) 1-9.

[18] V.B. Veljković , J.M. Avramović, O.S. Stamenković, Biodiesel production by ultrasound assisted transesterification: State of art and the perspectives, Ren. Sus. Energy Rev. 16 (2012) 1193-1209.

[19] P. Cintas, S. Mantegna, E. Calcio Gaudino, G. Cravotto, A new pilot flow reactor for high-intensity ultrasound irradiation. Application to the synthesis of biodiesel. Ultrason. Sonochem. 17 (2010) 985-989.

[20] C. Stavarache, M. Vinatoru, Y. Maeda, H. Bandow, Ultrasonically driven continuous process for vegetable oil, Ultrason. Sonochem. 14 (2007) 413-417.

[21] D.C. Boffito, S. Mansi, J.-M. Leveque, C. Pirola. C.L. Bianchi, G. Patience, Ultrafast biodiesel production suing ultrasound in batch and continuous reactors, Sus. Chem. Eng. 1(11) (2013) 1432-1439.

[22] J.A. Colucci, A. Jose, E.E. Borrero, F. Alape, Biodiesel from an alkaline transesterification reaction of soybean oil using ultrasonic mixing, J. Am. Oil Chem. Soc. 82(7) (2005) 525-530.

[23] A.P. Vyas, J.L.Verma, N. Subrahmanyam, A review on FAME production processes, Fuel 89 (2010), 1-9.

[24] F.F.P. Santos, L.J.B.L. Matos, S. Rodrigues, F.A.N. Fernandes, Optimization of the production of methyl esters from soybean waste oil applying ultrasound technology, Energy & Fuels 23 (2009) 4116–4120.

[25] H. Zou, M. Lei, Optimum process and kinetic study of Jatropha curcas oil pre-esterification in ultrasonic field, J. Taiwan Inst. Chem. Eng. 43 (2012) 730–735.

[26] F.F.P. Santos, J.Q. Malveira, M.G.A. Cruz, F.A.N. Fernandes, Production of biodiesel by ultrasound assisted esterification of Oreochromis niloticus oil, Fuel 89 (2010) 275–279.

[27] T.J. Mason, J.P. Lorimer, Sonochemistry, Theory, Applications and Uses of Ultrasound in Chemistry, Wiley, New York, 1988.

[28] B. Toukoniitty, J.P. Mikkola, D. Yu. Murzin, T. Salmi , Utilization of electromagnetic and acoustic irradiation in enhancing heterogeneous catalytic reactions, Appl. Catal. A 279 (2005) 1-22.

[29] L.H. Thompson, L.K. Doraiswamy, Sonochemistry: Science and engineering, Ind. Eng. Chem. Res. 38(4) (1999) 1215-1249.

[30] N. Kardos,J.L. Luche, Sonochemistry of cabohydrate compounds, Carbohydr. Res. 332(2) (2001) 115-131.

[31] N. Öezbay, N. Oktar, N.A. Tapan, Esterification of free fatty acids in waste cooking oils (WCO): role of ion-exchange resins, Fuel 87 (2008) 1789-1798.

[32] D. Barnabè, R. Bucchi, A. Rispoli, C. Chiavetta, P.L. Porta, C.L. Bianchi, C. Pirola, D.C. Boffito, G. Carvoli, Land use change impacts of biofuels: a methodology to evaluate biofuel

sustainability in: Z. Fang (Ed.), Biofuels - Economy, Environment and Sustainability, Intech, 2013, pp. 3-37.

[33] B. Redaelli, Innovative method via esterification for the abatement of acidity in vegetable oils for biodiesel production, Department of Chemistry, University of Milan, Master degree thesis, 2006.

[34] V. Ragaini, C. Pirola, S. Borrelli, C. Ferrari, I. Longo, Simultaneous ultrasound and microwave new reactor: detailed description and energetic considerations, Ultrason. Sonochem. 19 (2012), 872-876.

[35] J.M. Löning, C. Hors, U. Hoffmann, Investigation on the energy conversion in sonochemical processes, Ultrason. Sonochem. 2002, 9, 169.

[36] S. Pasias, N. Barakos, C. Alexopoulos, N. Papayannakos, Heterogeneously Catalyzed Esterification of FFAs in Vegetable Oils, Chem. Eng. Technol. 29 (2006) 1365-1371.

[37] D.C. Boffito, Biodiesel Production from Non-Edible Foodstuff: Chemistry, Catalysis and Engineering, Department of Chemistry, University of Milan, PhD thesis, 2013.

[38] R. Tesser, L. Casale, D. Verde. M. Di Serio, E. Santacesaria, Kinetics of free fatty acids esterification: batch and loop reactor modeling, Chem. Eng. J. 154 (2009) 25-33.

[39] R. Tesser, L. Casale, D. Verde. M. Di Serio, E. Santacesaria, Kinetics and modelling of fatty acids esterification on acid exchange resins. Chem. Eng. J. 157 (2010) 539-550.

[40] V.G. Deshmane, P.R. Gogate, A.B. Pandit, Ultrasound-Assisted Synthesis of Biodiesel from Palm Fatty Acid Distillate, Ind. Eng. Chem. Res. 48 (2009) 7923–7927.

[41] V.G. Deshmane, P.R. Gogate, A.B. Pandit, Ultrasound assisted synthesis of isopropyl esters from palm fatty acid distillate, Ultrason. Sonochem. 16 (2009) 345–350.

Tables and figures captions

Table 1. Fatty acids composition of the feedstocks. Cx:y indicates the number of carbons (x) and the total number on unsaturations in the chain (y). The number in brackets indicates the concentration of the fatty acid in $\%_{wt}$.

Table 2. Free fatty acids esterification experiments. Catalyst: Amberlyst®46.

Table 3. Features of Amberlyst®46.

Table 4. Best fit parameters estimates w/US and w/o US.

Figure 1. Sulphonic ion exchange resins of the Amberlyst®46 type.

Figure 2. Ultrasonic batch reactor (20 kHz).

Figure 3. Conversions w/US and w/o US at 63 °C. The lines represent the model.

Figure 4. Conversions w/US and w/o US at 40 °C. The lines represent the model.

Figure 5. Conversions w/US and w/o US of the tobacco seed oil. The lines represent the model.

Tobacco seed oil	C14:0 (2.0) C16:0 (8.3) C18:0 (1.5) C18:1 (12.0) C18:2 (75.3) C18:3 (0.6) C20:0 (0.1) C22:0 (0.2)
Canola oil	C16:0 (7.6) C18:0 (1.3) C18:1 (64.5) C18:2 (23.7) C18:3 (2.4) C20:0 (0.5)
Oleic acid	C18:1 (100)

Table 1

Test	Oil	Initial acidity ($\%_{wt}$)	Acid value (mg KOH g^{-1})	Process	Temp.
1	Canola	4.2-4.6*	5.9-6.5	conventional	40 °C
2					63 °C
3				US	40 °C
4					63 °C
5	Tobacco	1.2	1.7	conventional	20 °C
6					40 °C
7					63 °C
8				US	20 °C
9					40 °C
10					63 °C
11	Oleic acid	100	142	conventional	63 °C
12				US	63 °C

Table 2

Catalyst A46	
Cross-linking degree	medium
Surface area ($m^2\ g^{-1}$)	75
Ave. D_p (Å)	235
Total V_p (ccg^{-1})	0.15
Declared Acidity (meq H^+g^{-1})	0.43
Moisture content ($\%_{wt}$)	26-36
Shipping weight (g l^{-1})	600
Max. operating T (°C)	120

Table 3

Feedstock	ppm H_2O	T °C	k $L^2mol^{-1}min^{-1}$	K_{Eq}	k_m $L\,min^{-1}$	$k_{m,US}$ $L\,min^{-1}$	$k_{m,US}/k_m$	k_{H2O} $L\,min^{-1}$	R^2	R^2_{US}
Oleic acid	0	63	0.0050	0.57	0.0034	0.0064	1.9	0.06	1.00	1.00
Canola	600	40	0.0009	0.073	0.0015	0.0040	2.6	0.05	0.98	0.97
Canola	600	63	0.0088	0.380	0.0017	0.0020	1.2	0.02	0.99	0.99
Tobacco	2000	20	0.0005	0.007	0.0004	0.0024	6.7	0.02	0.99	0.97
Tobacco	2000	40	0.0003	0.027	0.0019	0.0080	4.1	0.02	1.00	0.98
Tobacco	2000	63	0.0027	0.050	0.0013	0.0026	2.0	0.01	0.99	0.98

Table 4.

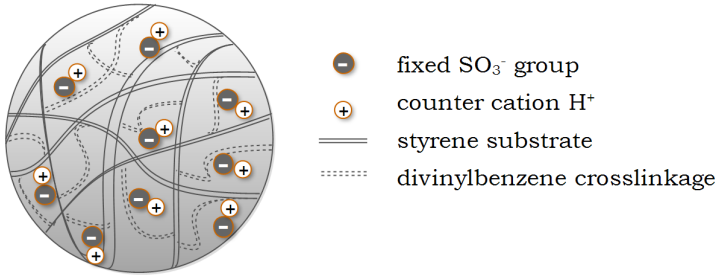
fixed SO_3^- group
counter cation H^+
styrene substrate
divinylbenzene crosslinkage

Figure 1

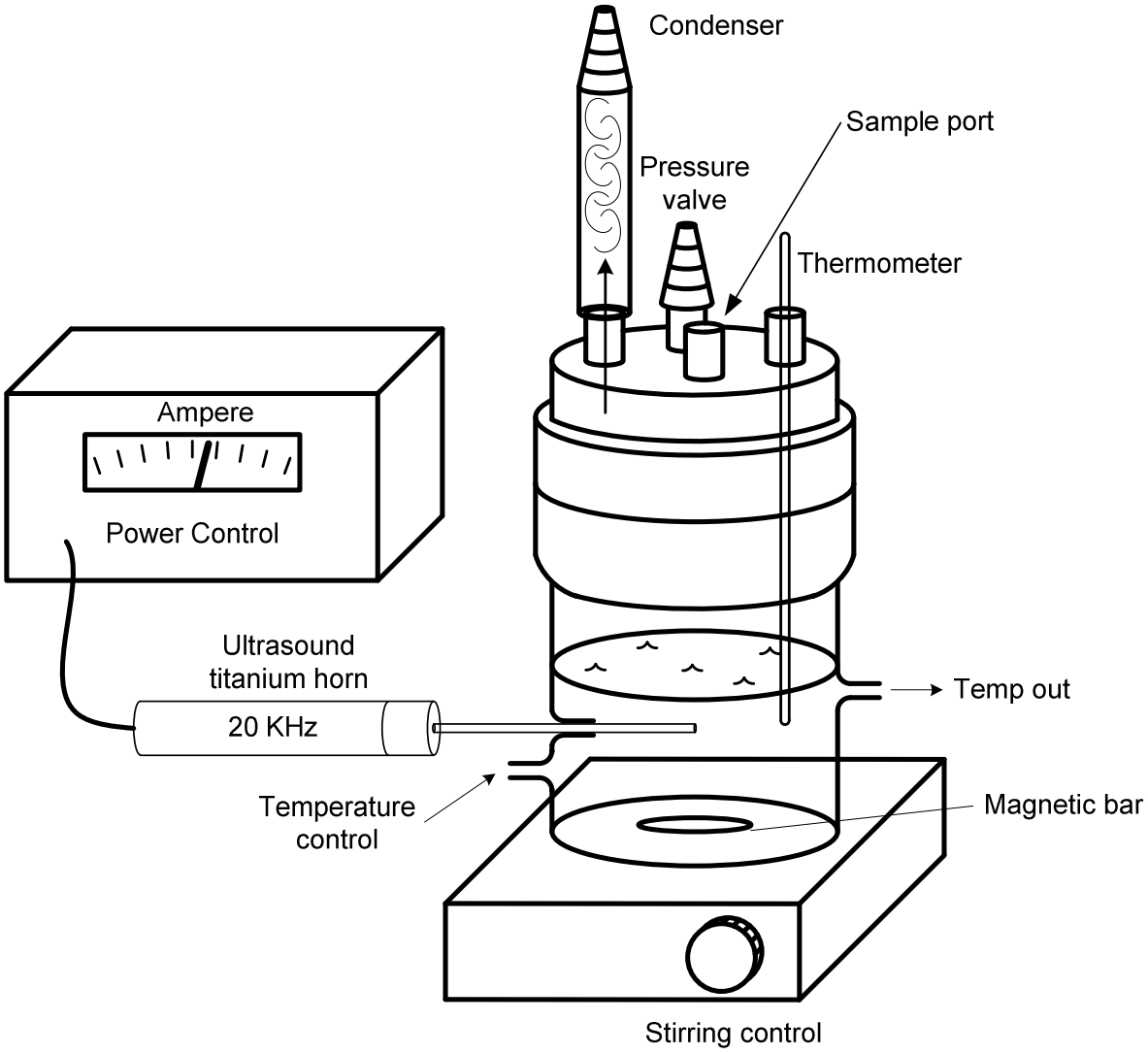
Condenser
Sample port
Pressure valve
Thermometer
Ampere
Power Control
Ultrasound titanium horn
20 KHz
Temp out
Temperature control
Magnetic bar
Stirring control

Figure 2

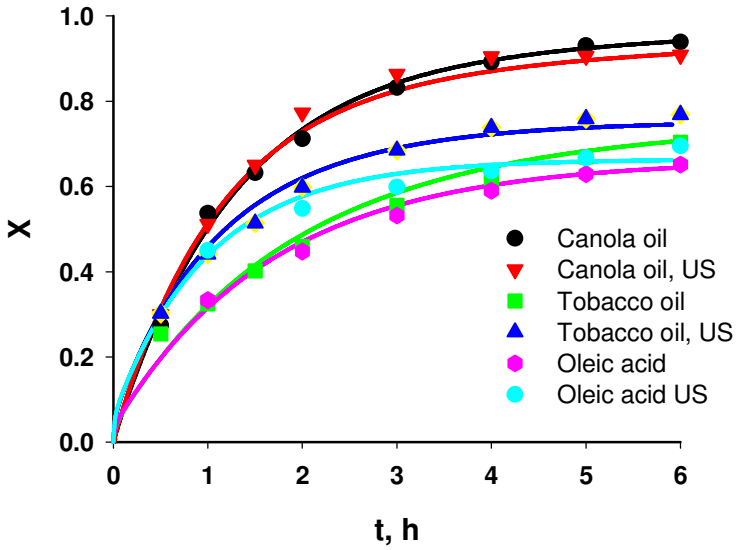
1.0
0.8
0.6
0.4
0.2
0.0
X
0
1
2
3
4
5
6
t, h
Canola oil
Canola oil, US
Tobacco oil
Tobacco oil, US
Oleic acid
Oleic acid US

Figure 3

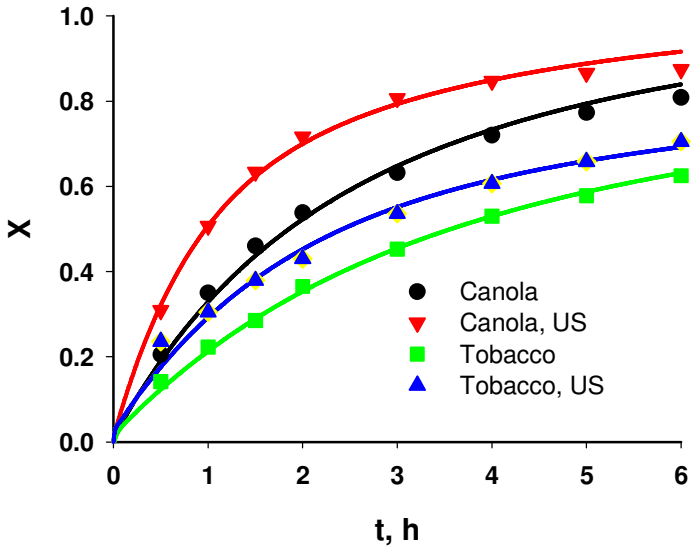
1.0
0.8
0.6
0.4
0.2
0.0
X
0
1
2
3
4
5
6
t, h
Canola
Canola, US
Tobacco
Tobacco, US

Figure 4

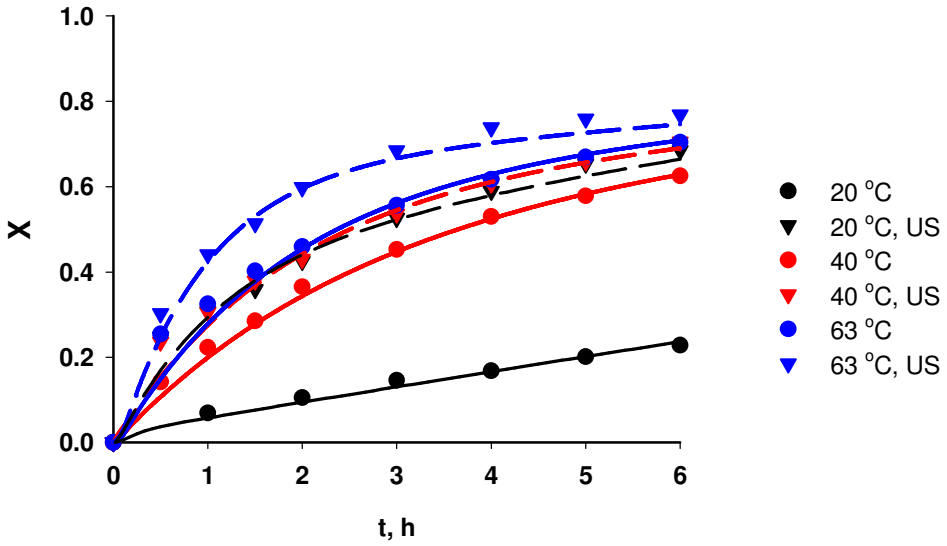

Figure 5